Exploring the Crucial Role of Atmospheric Carbonyl Compounds in Regional Ozone heavy Pollution: Insights from Intensive Field Observations and Observation-based modelling in the Chengdu Plain Urban Agglomeration, China

Jiemeng Bao[1,2], Xin Zhang[1,2], Zhenhai Wu[1], Li Zhou[3], Jun Qian[4], Qinwen Tan[5], Fumo Yang[3], Junhui Chen[6], Yunfeng Li[7], Hefan Liu[5], Liqun Deng[6], Hong Li[1*]

[1]Chinese Research Academy of Environmental Sciences, State Key Laboratory of Environmental Benchmarks and Risk Assessment, Beijing 100012, China

[2]School of Environmental Science and Engineering of Peking University, State Key Joint Laboratory of Environmental Simulation and Pollution Control, Joint Laboratory of Regional Pollution Control International Cooperation of the Ministry of Education, Beijing 100871, China

[3]College of Carbon Neutrality Future Technology, Sichuan University, Chengdu 610065, China

[4]Sichuan Radiation Environment Management and Monitoring Central Station, Chengdu 611139, China

[5]Chengdu Academy of Environmental Sciences, Chengdu 610046, China

[6]Sichuan Academy of Eco-Environmental Sciences, Chengdu 610042, China

[7]School of Mechanical Engineering, Beijing Institute of Petrochemical Technology, Beijing 102617,China

Correspondence to: Hong Li (lihong@craes.org.cn)

Abstract. Gaseous carbonyl compounds serve as crucial precursors and intermediates in atmospheric photochemical reactions, significantly contributing to ambient ozone formation. To investigate the impact of gaseous carbonyls on regional ozone pollution, simultaneous field observations and observation-based modelling of ambient carbonyls were conducted at nine sites within the Chengdu Plain Urban Agglomeration (CPUA), China during August 4-18, 2019, when three episodes of regional heavy ozone pollution occurred across eight cities within CPUA. Throughout the study, the total mixing ratios of 15 carbonyls ranged from 10.70±4.16 to 35.18±13.37 ppbv, in which formaldehyde (48.1%), acetone (19.9%), and acetaldehyde (17.5%) were most abundant within the CPUA. Ambient levels of carbonyls and ozone showed some positive correlations in space (especially pronounced around Chengdu in both northern and southern directions)

31 and in diurnal variations with higher concentrations of carbonyls during ozone pollution

32 episodes. Photochemical reactivity analysis emphasized the significant contributions of

33 carbonyls, especially formaldehyde and acetaldehyde, to ozone formation. Sites with

34 higher average ozone concentrations during observations were mainly in the VOCs-

35 limited regime, while others were in the transitional regime. Local primary emissions,

36 mutual air transportation among cities within the CPUA and photochemical secondary

37 processes were recognized to contribute significantly to the production or the

38 contamination of carbonyls in ambient air, with alkenes and alkanes being important

39 precursors of secondary carbonyls. This study highlights the pivotal role of carbonyls

40 in heavy ozone pollution within the CPUA, China, providing valuable scientific insights

41 to guide the development of effective countermeasures for regional ozone pollution

42 control in the future.

43 **Keywords:** Gaseous Carbonyls; Ozone Heavy Pollution; Pollution Characteristics;
44 Atmospheric Photochemical Reactivity; Source Analysis; The Chengdu Plain Urban
45 Agglomeration, China

1. Introduction

47 Atmospheric carbonyl compounds play a pivotal role in tropospheric chemistry,

48 acting as crucial precursors to both ozone (O_3) and secondary organic aerosols (SOA),

49 a fact recognized for decades (Altshuller, 1993; Grosjean and Seinfeld, 1989). Their

50 importance has been confirmed by numerous studies over the years(Guo et al., 2004;

51 Hallquist et al., 2009; Wang et al., 2020; Ye et al., 2021; Coggon et al., 2019),

52 highlighting their significant contribution to atmospheric photochemistry and air

53 pollution. Over the past two decades, severe air pollution in China has driven substantial

54 research efforts to understand the contributions of carbonyl compounds to these

55 environmental challenges. Studies have shown that photolysis of carbonyl compounds

56 is a major source of RO_X radicals (Grosjean and Seinfeld, 1989; Zhang et al., 2016).

57 These compounds can be photolyzed and react with OH radicals to form a large number

58 of HO_2 and RO_2 radicals, which increase the atmospheric oxidation capacity and

59 participate in the NOx photochemical cycle, leading to ozone formation (Zhang et al.,

60 2016; Meng et al., 2017). Additionally, dialdehydes such as glyoxal and methylglyoxal

61 undergo heterogeneous reactions with aqueous particulate matter, rapidly forming SOA

62 (Lou et al., 2010; Xue et al., 2016; Yuan et al., 2012). Ambient carbonyl compounds

63 not only affect the environment but also pose direct health risks to humans. They can

64 harm ecosystems through deposition and adsorption processes (Yang et al., 2018). They

65 also pose direct health risks to humans, including sensitization, carcinogenesis, and

66 mutagenicity (Fuchs et al., 2017).

67   Recent research has increasingly focused on understanding the spatial and

68 temporal variability of carbonyl compounds in highly polluted regions, particularly in

69 China, where rapid industrialization has led to severe air quality challenges. Xue et al.

70 (2013) and Duan et al. (2012) reported typical ambient concentrations of carbonyl

71 compounds ranging from a few $\mu g \cdot m^{-3}$ to tens of $\mu g \cdot m^{-3}$ in urban areas, depending on

72 the specific compounds and regions studied. For example, formaldehyde concentrations

73 in highly polluted areas can exceed 10 $\mu g \cdot m^{-3}$. Shen et al. (2013) and Fu et al. (2008)

74 observed significant diurnal variation, with higher concentrations of carbonyl

75 compounds during the daytime, particularly in the afternoon, driven by photochemical

76 production. Concentrations can increase by as much as 50-100% during peak sunlight

77 hours compared to nighttime levels. Pang and Mu (2006) and Rao et al. (2016)

78 identified key sources of carbonyl compounds, including vehicular emissions, industrial

79 activities, and secondary formation from VOC oxidation in the atmosphere. In urban

80 environments, vehicular emissions are often a dominant primary source, while

81 secondary formation contributes significantly during daytime due to photochemical

82 processes. The results highlight severe and spatiotemporal variations of carbonyl

83 pollution in China. High levels are found mainly in the North China Plain(NCP), the

84 Yangtze River Delta(YRD), and the Pearl River Delta(PRD)(Duan et al., 2008; Shao et

85 al., 2009; Tan et al., 2018; Wang et al., 2018; Xue et al., 2014, 2013; Yang et al., 2017).

86 Urban areas generally exhibit higher carbonyl levels than suburban and rural areas due

87 to human activities(Xue et al., 2013). Despite the progress made, significant gaps

88 remain in understanding the spatiotemporal distribution and source apportionment of

89 carbonyl compounds, particularly in urban agglomerations. Existing research has

90 primarily focused on urban areas in rapidly developing regions like the NCP, YRD, and

91 PRD. Moreover, studies have often emphasized the overall role of VOCs in ozone

92 pollution, with less attention given to specific carbonyl compounds and their individual

93 contributions to atmospheric oxidation capacity and ozone formation (Meng et al.,

94 2017).

95   Monitoring carbonyl compounds in the atmosphere is challenging due to their

96 typically low concentrations (ppt-ppb levels), necessitating highly sensitive analytical

97 methods. The diversity of carbonyl compounds, including multiple isomers, requires

98 highly selective analytical techniques for differentiation. Current measurement

99 technologies limit our understanding of the spatiotemporal distribution of carbonyl

100 compounds, affecting the accurate assessment of their environmental behavior, sources,

101 and transport (Xue et al., 2013; Sahu and Saxena, 2015). While numerous studies have

102 explored the role of carbonyl compounds in ozone production, many focus on general

103 mechanisms rather than specific compounds or regional variations (Atkinson and Arey,

104 2003; Monks et al., 2015).

105   Atmospheric carbonyl compounds originate from both primary and secondary

106 sources (Pang and Mu, 2006; Rao et al., 2016). Primary sources include the incomplete

107 combustion of fossil fuels and biomass, industrial emissions, emissions from the

108 catering industry, and releases from plants. Secondary sources arise from the

109 atmospheric photochemical oxidation of VOCs (Xue et al., 2013), particularly

110 alkenes, aromatics, and isoprene, which typically dominate the secondary formation of

111 carbonyls. However, distinguishing between primary and secondary contributions

112 remains challenging. Existing source apportionment methods, such as characteristic

113 species ratios and multiple linear regression, often lack the resolution to differentiate

114 these sources accurately, especially for non-vehicular emissions and secondary

formation. The limitations of these methods underscore the need for more advanced approaches to better quantify the secondary formation mechanisms of carbonyl compounds and their regional impact on ozone formation. Despite significant advancements in studying atmospheric carbonyls, key gaps remain in understanding their precise spatiotemporal distribution and source apportionment. Specifically, there is a need for studies that examine how carbonyls vary across different environments—urban, suburban, and rural—and during varying pollution events. Without such targeted analysis, our understanding of the behavior of carbonyl compounds and their contribution to ozone pollution remains incomplete, particularly in regions experiencing severe pollution.

In this context, this study focuses on atmospheric carbonyl compounds and their roles in photochemical pollution within the Chengdu Plain Urban Agglomeration (CPUA) of China. The CPUA includes eight cities: Chengdu, Mianyang, Deyang, Leshan, Meishan, Yaan, Suining, and Ziyang. This region has a developed economy and a high degree of internationalization. The CPUA is located on the western edge of the Sichuan Basin, surrounded by mountain ranges, which easily block airflow. The unique climatic environment of the CPUA features low wind speeds year-round, high frequency of static winds, short hours of sunshine, frequent winter inversions, and a pronounced heat island effect in summer. These climatic characteristics significantly impact the variations in air pollutant concentrations, making the region prone to ozone pollution in summer and haze pollution in winter. (Li et al., 2013; Hu et al., 2017; Zhang et al., 2010). Although previous studies have shown that ozone formation in urban Chengdu is primarily VOCs-limited (Tan et al., 2018), with aromatic hydrocarbons and alkenes contributing significantly to ozone generation in summer (Xu et al., 2020), these studies mainly focus on single cities and overall VOCs. There is limited understanding of the distribution, sources, and specific roles of carbonyl compounds across the entire CPUA and their contributions to regional ozone pollution and mutual air transport mechanisms.

143   To address these research gaps, this study involves an intensive field observation

144   experiment conducted by the Sichuan Academy of Environmental Sciences, Peking

145   University, Sichuan University and Chinese Academy of Environmental Sciences.

146   Atmospheric carbonyl compounds were observed at nine sites in eight cities within the

147   CPUA for 15 days during a period of heavy ozone pollution in August 2019. Samples

148   were analyzed using 2,4-dinitrophenylhydrazine solid phase adsorption/high

149   performance liquid chromatography (HPLC). The study aims to characterize the

150   atmospheric carbonyl compounds in the CPUA, assess their influence on

151   photochemical pollution, identify key carbonyl compounds that may play crucial roles

152   in heavy ozone pollution in the CPUA, and evaluate the contribution of primary

153   emissions, air pollution transport, and secondary generation to key carbonyl compounds

154   through a combination of multivariate linear regression modeling and Observation-

155   Based Modeling (OBM). This research aims to provide technical support for controlling

156   carbonyl compounds pollution in the CPUA and to reduce their contributions to ozone

157   pollution.

158   **2. Materials and methods**

159   **2.1 Observation Sites Profile**

160   In this study, a total of 9 off-line sampling sites for atmospheric carbonyl

161   compounds were set up in 8 cities in the CPUA from August 4th to 18th, 2019(table S1).

162   Considering that this study focused on the pollution characterization of carbonyl

163   compounds in urban areas, one urban site was selected in each city. In addition, in order

164   to compare and study the pollution characteristics of carbonyl compounds in the

165   suburbs, a suburban site was set up in Xinjin County, Chengdu. For the selection of

166   urban sites in each city, priority is given to those choices of set-up in the vicinity of the

167   state-controlled site, and the perimeter of the sites should be open, unobstructed and no

168   obvious pollution sources, with convenient transportation and power supply. The

169   distribution of specific sites is shown in Fig. 1.

170   Ozone concentrations were measured using the UV absorption method with a

171   Thermo O_3 analyzer (Model 49i), with data sourced from national control stations near

172   each sampling site. Nitrogen dioxide (NO_2) was measured by chemiluminescence

173   following chemical conversion to nitric oxide (NO) using a molybdenum catalyst;

174   however, this method is known to have interferences from other NOz species. Carbon

175   monoxide (CO) was measured via infrared absorption with a Thermo instrument

176   (Model 20). All Thermo instruments were carefully maintained and calibrated daily at

177   01:00 to ensure measurement accuracy. Measurements for ozone, NO_2, and CO were

178   collected with a time resolution of one hour. Simultaneously, meteorological

179   parameters—temperature, relative humidity (RH), wind speed, and direction—were

180   recorded at each observation site using an automatic weather station (PC-4, JZYG,

181   China), also at a one-hour resolution.
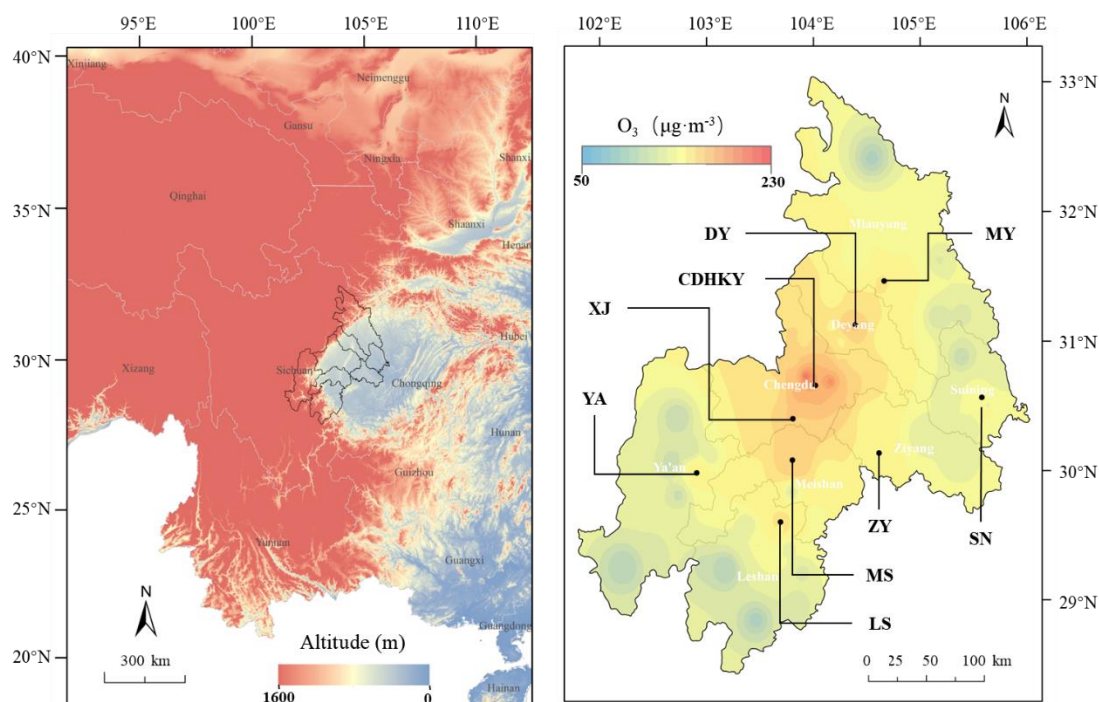
183   **Figure 1.** Distribution of sampling sites. The left panel shows the elevation map of the Sichuan

184   Basin, highlighting the geographical features of the region, with elevation data sourced from the

185   Geospatial Data Cloud (https://www.gscloud.cn/#page1/2). The right panel presents the spatial

186   distribution of ozone concentrations in the CPUA during the observation period (August 4–18,

187   2019), with ozone data obtained from national control stations near each sampling site. Black dots

188   represent the locations of the sampling sites, labeled as follows: MY (Mianyang), DY (Deyang),

189   CDHKY (Chengdu Environmental Science Research Institute), XJ (Xinjin), SN (Suining), ZY

190 (Ziyang), MS (Meishan), YA (Ya'an), and LS (Leshan). The color bar in the top left corner
191 corresponds to interpolated ozone concentrations, with each color representing a concentration
192 gradient.

193 **2.2 Samples Collection**

194   The sampling of atmospheric carbonyl compounds mainly referred to the TO-11A

195 standard of the United States Environmental Protection Agency (US EPA) and the

196 Chinese environmental protection standard HJ 683-2014 High Performance Liquid

197 Chromatography Method for the Determination of Atmospheric Carbonyl Compounds,

198 and the sampling was carried out by using silica gel sampling tubes (IC-DN3501 from

199 Tianjin Bonna-Agela) coated with DNPH (2,4-dinitrophenylhydrazine). In this study,

200 an automatic sampler for carbonyl compounds (Zhang et al., 2019) was used to

201 continuously collect atmospheric carbonyl compounds. From August 4th to 18th, 2019,

202 air samples were collected every 2 hours with a sampling flow rate of $0.8 \; L \cdot min^{-1}$. In

203 addition, in order to prevent the impact of ozone and rainwater in the atmospheric air

204 on sample collection, a potassium iodide ozone removal column (KI 140 from Tianjin

205 Bonna-Agela) was installed and a water removal agent made by ourselves (Bao et al.,

206 2022; Wang et al., 2020) was added at the front end of the sample tube. Two blank

207 samples were collected before and after the sampling, and blank samples were also

208 collected for different batches of sampling tubes. The samples were frozen at -18°C and

209 analyzed within one month.

210   Atmospheric VOCs were sampled using SUMMA tanks, stainless steel tanks with

211 electropolished and silanized inner walls, manufactured by Entech in the United States,

212 with a sampling volume of 3.2 liters. The sampling was controlled by a constant current

213 integral sampler to sampling for an average of 1 hour. From August 4th to 18th, 2019,

214 two VOCs samples were collected each day at each site, at 8:00-9:00 and 14:00-15:00

215 (no samples were taken under special weather conditions, such as rain). On August 11th,

216 12th and 16th , six samples were collected per day to capture diurnal variations under

217 ozone pollution events, at the following times: 8:00-9:00, 10:00-11:00, 12:00-13:00,

218 14:00-15:00, 16:00-17:00, and 18:00-19:00.

 2.3 Samples Analysis

220   The carbonyl compounds samples were qualitatively and quantitatively analyzed

221 by using High Performance Liquid Chromatography (HPLC) (LC-20AD, Shimadzu,

222 Japan) and an ultraviolet detector (SPD-20A, Shimadzu, Japan), mainly based on the

223 US EPA TO-11A standard and the Chinese HJ 683-2014 standard. The DNPH sampling

224 column after sampling was slowly eluted into a volumetric flask using acetonitrile

225 (chromatographically pure, Thermo Fisher Scientific China) to 5.0 mL. Then 1.5 mL

226 sample was taken into an HPLC sample bottle, and sealed and stored in a refrigerator

227 at <4 °C to complete the pre-treatment. Prior to sample analysis, a standard solution of

228 the concentration gradient was prepared using TO-11A standard solution (Supelco,

229 USA) and used as the external standard. The correlation coefficient (R^2) of the standard

230 curve was greater than 0.995. The limit of detection of the device was 0.56~5.57

231 $ng·mL^{-1}$, and the limit of quantification was 1.87~18.56 $ng·mL^{-1}$ (Table S2). Then 20

232 μL of the pretreated sample was extracted through the autosampler and injected into the

233 HPLC/UV system, detected by a UV detector with a wavelength of 360 nm, qualified

234 by retention time value, quantified by peak area value, and the qualitative and

235 quantitative analysis data of carbonyl compounds were obtained after conversion. The

236 HPLC conditions referred to Chinese environmental protection standard HJ 683-2014:

237 binary gradient washing was performed using acetonitrile and water, 60% acetonitrile

238 was held for 20 mins, acetonitrile was increased linearly from 60% to 100% within 20-

239 30 mins, and acetonitrile was reduced to 60% again within 30-32 mins and held for 8

240 mins; the column oven was kept at 40 °C.

241   The atmospheric VOCs were analyzed using the TO-14 and TO-15 methods,

242 which are recommended by the US EPA. These methods involve frozen

243 preconcentration coupled with gas chromatography and mass spectrometry (GC-MS).

244 TO-15 is a method for detecting and quantifying a wide range of VOCs from air samples.

245 The VOCs were pre-concentrated by the Entech7100 system at a low temperature, then

246 quantified by an Agilent GC-MS. During the sample analysis, four internal standard

247 gases (bromochloromethane, 1,4-difluorobenzene, chlorobenzene-d5, and 4-

248 bromofluorobenzene) were used. A multi-point calibration curve was created using a

249 standard gas containing 118 VOCs, including PAMS compounds, TO-15 target analytes,

250 and carbonyl compounds. PAMS (Photochemical Assessment Monitoring Stations)

251 compounds are a subset of hydrocarbons known to contribute to ozone formation, such

252 as ethane, ethylene, propane, and others."

253 **2.4 Data Analysis**

254 **2.4.1 Ozone pollution assessment criteria**

255 According to the Technical Regulation on Ambient Air Quality Index (on trial),

256 National Environmental Protection Standard of the People's Republic of China HJ

257 633—2012, days with an ozone pollution index (IAQI) of 100 or higher during the

258 observation period were designated as pollution days, while days with an IAQI below

259 100 were considered clean days. This study compared the pollution characteristics of

260 carbonyl compounds between pollution days and clean days. Additionally, the

261 concentrations of formaldehyde, acetaldehyde, and acetone observed during the

262 summer of 2009-2013 in economically developed and industrialized areas such as

263 Beijing, Shanghai, and Guangzhou in China, as well as locations in South America

264 (Brazil), Asia (Thailand), Europe (France), and North America (United States), were

265 selected and compared.

266 **2.4.2 Ozone formation sensitivity**

267 Previous studies have shown that the formaldehyde to NO_2 ratio (FNR) can be

268 used to determine the sensitivity of O_3-NOx-VOCs (Schroeder et al., 2017; Tonnesen

269 and Dennis, 2000; Vermeuel et al., 2019). Most studies used satellite remote sensing-

270 based FNR, but the FNR column concentration ratios inverted by satellite remote

271 sensing mainly represented the average photochemical of the troposphere, and the

272 concentration distributions of HCHO and NO_2 in the vertical direction were

273   inconsistent (Hong et al., 2022; Schroeder et al., 2017). So, there is a large uncertainty

274   to develop ground-level ozone pollution prevention and control measures. In this study,

275   sensitivity analysis of ground-level ozone formation was carried out based on the ratio

276   of ground-level HCHO to NO_2 during the observation period at the 9 sites of 8 cities in

277   the CPUA. FNR < 0.55±0.16 and FNR > 1.0±0.3 were defined to VOCs-limited and

278   NOx-limited, respectively, and FNR ratio ranged from 0.55±0.16 to 1.0±0.3 defined to

279   NO_X and VOCs co-limited (Liu et al., 2021; Zhang et al., 2022).

280   **2.4.3 Exploration of Secondary Formation Mechanisms**

281   **(1) Atmospheric chemical reactivity**

282   In this study, the contribution of atmospheric chemical reactivity of carbonyl

283   compounds to ozone formation was evaluated using the OH free radical consumption

284   rate (L_{OH}) and ozone formation potential (OFP):

$$L_{OH} = [OVOC]_i \times k_i(OH) \tag{1}$$

286   Where, $[OVOC]_i$ was the observed concentration of the ith (i=1 to n) carbonyl

287   compound, in molecule·cm^{-3}; $k_i(OH)$ was the rate constants of the ith carbonyl

288   compound reacting with OH radicals, in cm^3·(molecule·s)$^{-1}$. The unit of L_{OH} is s^{-1},

289   representing the rate of OH radical consumption. The selected $k_i(OH)$ values were from

290   literature (Atkinson and Arey, 2003).

$$OFP = MIR_i \times [OVOC]_i \tag{2}$$

292   Where, MIR was the maximum incremental reactivity of the ith carbonyl

293   compound,in g O_3·(g VOC)$^{-1}$ (grams of ozone formed per gram of volatile organic

294   compound), and the MIR values of each species were from California Code of

295   Regulations (https://govt.westlaw.com); $[OVOC]_i$ was the mass concentration of the ith

296   carbonyl compound, in μg·m^{-3}. The unit of OFP is μg·m^{-3}, representing the potential

297   ozone formation.

298   **(2) Observation-based model (OBM)**

299   The Observation-Based Model (OBM) is a box model that uses actual

300   observational data to evaluate the sensitivity of secondary pollutant formation

301   mechanisms to their precursor emissions. By constraining the model with atmospheric

302   observation data, typical secondary pollutants and parameters such as NO_X, SO_2, CO,

303   VOCs, temperature, humidity, pressure, and JNO_2 are input into the model as hourly

304   observational data to calculate the chemical formation and consumption of secondary

305   pollutants and free radicals. In this study, the OBM model used the Master Chemical

306   Mechanism (MCM) (v3.3.1, mcm.leeds.ac.uk), which is a nearly detailed chemical

307   mechanism that describes the chemical processes of 143 VOC species from emission

308   to degradation in the atmosphere, including approximately 6,700 species and 17,000

309   inorganic and organic reactions. The MCM chemical mechanism can simulate

310   atmospheric photochemical reaction processes under near-real conditions and calculate

311   the concentrations of highly reactive species, quantifying the reaction rates of all

312   species involved.

313   Relative Incremental Reactivity (RIR) was first used by Cardelino and Chameides

314   (1995) to simulate the response of ozone to precursor changes through scenario tests

315   using box model calculations. RIR was calculated by assuming that the concentration

316   of a given carbonyl compound precursor decreased by a certain proportion could cause

317   the change of the concentration of the carbonyl compound, so as to further judge the

318   effect of VOCs on the formation of carbonyl compounds. Combining the concentrations

319   and activity levels of 15 carbonyl compounds during the observation period, this study

320   focused on formaldehyde, acetaldehyde, and acetone as the primary research targets.

321   The impacts of various AVOCs(anthropogenic VOCs), including alkanes, alkenes,

322   alkynes, and aromatic hydrocarbons, as well as BVOCs(biogenic VOCs)like isoprene,

323   on the formation of formaldehyde, acetaldehyde, and acetone were assessed using

324   observation-based OBM classification. Specific species of anthropogenic source VOCs

325   (alkanes, alkenes, alkynes, and aromatic hydrocarbons) and biogenic VOCs (isoprene)

326   are detailed in Table S3.

327   VOCs observations, conventional gases (NO_2, CO and SO_2) and meteorological

328   parameters (temperature, relative humidity and pressure) were imputed into the model.

329   It was assumed that the pollutants are well mixed. Under the constraints of the measured

330   hourly concentration data of pollutants, the atmospheric chemical process was

331   simulated to obtain the source-effect relationship of the measured pollutants. By

332   assuming the reduction of the source effect, the RIRs of different carbonyl compounds

333   precursors were calculated, and the sensitivities of carbonyl compounds to different

334   pollutants were obtained, and then the secondary formation mechanism of carbonyl

335   compounds was determined. The formula to calculate the RIR is as follows:

336    $$RIR(X) = \left[\frac{\Delta P_Y(X)/P_Y(X)}{\Delta S(X)/S(X)}\right] \qquad (3)$$

337    $$P_Y = Y_{\text{net formation}} - Y_{\text{net consumption}} \qquad (4)$$

338   Where X was a specific species; $P_Y(X)$ was the net formation rate of species y;

339   S(X) was the total amount of emissions of species X in a certain period, i.e., the source

340   effect of species X. $\Delta S(X)$ was the change in total emissions of X caused by the

341   hypothetical change in source effect, $\Delta P_Y(X)$ was the change in $P_Y(X)$ after the change

342   in source effect S(X), and RIR(X) was the relative incremental reactivity of species X.

343   The species Y in this study were formaldehyde, acetaldehyde and acetone, respectively,

344   and pollutant X was reduced by 20%.

345   The absolute RIR of the precursor reflects the sensitivity of carbonyl compounds

346   formation to the precursor. The higher the absolute RIR, the more sensitive the carbonyl

347   compounds formation to the precursor. A positive RIR value indicates that reducing the

348   species can reduce the formation rate of species Y, and a negative RIR value indicates

349   that reducing the species can increase the formation rate of species Y.

350   **2.4.4 Sources Analysis**

351   **(1) Multi-linear regression model**

352   There is a good correlation between concentrations of compounds of the same or

353 similar source in the atmosphere. Based on this property, it was assumed that the

354 primary and secondary sources of carbonyl compounds were linearly correlated with

355 the selected tracers, and then a quantitative source model was established by multiple

356 linear statistical regression analysis (Kanjanasiranont et al., 2016a; Li et al., 2010; Ling

357 et al., 2017; Luecken et al., 2012; Lui et al., 2017; Wang et al., 2017). In general, CO is

358 the marker product of typical anthropogenic combustion source emissions, mainly from

359 vehicle exhaust emissions and coal combustion. Ozone, as an indicator of

360 photochemical smog, is a typical secondary formation pollutant. In this study, CO and

361 ozone were selected as the tracers of primary source and secondary source of carbonyl

362 compounds, respectively. The formula is as follows:

363
$$[carbonyl] = \beta_0 + \beta_1[CO] + \beta_2[O_3] \tag{6}$$

364 Where [carbonyl], [CO] and [O_3] represented the observed mixing ratios of

365 carbonyl compounds, CO and ozone, respectively, in ppbv. β_0, β_1 and β_2 were

366 coefficients obtained by multiple linear regression fitting model, in ppbv/ppbv. β_0

367 represented the background concentration of a given carbonyl compound, β_1

368 represented the emission ratio of the carbonyl compound relative to CO. $\beta_1[CO]$ and

369 $\beta_2[O_3]$ represented the concentrations of carbonyl compound in primary emission and

370 secondary formation, respectively, in ppbv.

371 In addition, the relative contribution of primary emissions, secondary formation

372 and background concentrations of carbonyl compounds can be calculated using the

373 following formula:

374
$$P_{primary} = \frac{\beta_1[CO]_i}{(\beta_0 + \beta_1[CO]_i + \beta_2[O_3]_i)} \times 100\% \tag{7}$$

375
$$P_{secondary} = \frac{\beta_2[O_3]_i}{(\beta_0 + \beta_1[CO]_i + \beta_2[O_3]_i)} \times 100\% \tag{8}$$

376
$$P_{background} = \frac{\beta_0}{(\beta_0 + \beta_1[CO]_i + \beta_2[O_3]_i)} \times 100\% \tag{9}$$

377 Where, $P_{primary}$ represented the contribution of the primary emission of a given

378 carbonyl compound, %; $P_{secondary}$ represented the contribution of the secondary

379 formation of the carbonyl compound species, %; $P_{background}$ represented the contribution

380 of the carbonyl compounds species from sources other than primary emissions and

381 secondary formation, %.

382 **(2) Backward trajectory model**

383 The effects of long-distance air mass transport on the pollution of carbonyl

384 compounds in the CPUA were studied using MeteoInfo software and TrajStat plug-in

385 (http://www.meteothink.org/downloads/index.html). In this model, meteorological

386 data were relevant meteorological data from the global date assimilation system (GDAS)

387 database (ftp://arlftp.arlhq.noaa.gov/pub/archives/gdasl). A trajectory simulation height

388 of 500 m was selected. The duration of backward trajectory was 48 h. The daily start

389 time was 00:00 UTC. The analog frequency was 2 h. The backward trajectory diagram

390 was calculated. Meanwhile, the clustering method in TrajStat software and the

391 Euclidean distance algorithm were used to cluster the airflow trajectory to the CPUA.

392 And then the statistical analysis was carried out in combination with the corresponding

393 pollutant mass concentration characteristics.

394 **3. Results and Discussion**

395 **3.1 Overview of air quality during observation period**

396 Due to the influence of cooling and precipitation caused by cold air intrusion, the

397 early observation period (from August 4th to 6th, 2019) in the Chengdu Plain Urban

398 Agglomeration (CPUA) experienced slightly lower temperatures (25.1°C) and higher

399 humidity (87.6%). These conditions were unfavorable for ozone formation. Although

400 ozone itself is not easily removed by rain, precipitation reduces ozone pollution by

401 washing away its precursors, such as nitrogen oxides (NOx) and volatile organic

402 compounds (VOCs), decreasing sunlight exposure, and enhancing atmospheric

403 dispersion. However, as temperatures increased and humidity dropped in the

404 subsequent days, more favorable conditions for ozone formation emerged, leading to

405 heavy and persistent regional ozone pollution in the CPUA. By August 12th, the mean

406 temperature had gradually increased to 29.1°C, while it averaged 27.7°C from August

407 13th to 14th. During this time, cumulative precipitation reached 975 mm, resulting in

408 temporary alleviation of ozone pollution. Subsequently, temperatures rose again from

409 August 15th to 18th, with the mean temperature persisting above 28.4°C for several days,

410 accompanied by a decrease in humidity to a minimum of 64.8% on August 17th. Overall,

411 during the observation period (from August 4th, 2019, 0:00 to August 18th, 2019, 24:00),

412 three episodes of severe ozone pollution occurred, namely EP1 (August 7th to 9th), EP2

413 (August 10th to 13th), and EP3 (August 15th to 18th), as depicted in Fig. 2.

414 Fig.3 illustrates the temporal and spatial variations of ozone and NO_2

415 concentrations, as well as temperature and humidity at each site during the observation

416 period. After observing the spatial distribution of ozone concentration during EP1, it's

417 evident that the severity of pollution reached heavily polluted levels, with Chengdu

418 recording an MDA8 concentration of 297 μg·m^{-3} on August 7th. This distribution

419 demonstrated a radial decrease from Chengdu to the surrounding areas. However, the

420 subsequent episodes, EP2 and EP3, exhibited even broader ranges of ozone pollution

421 and more pronounced spatial movements. During the early stages of EP2 and EP3 (from

422 August 10th to 11th and from August 14th to 15th, respectively), high ozone

423 concentrations were observed in the Chengdu-Deyang-Mianyang region. In the middle

424 stages (August 12th and from August 16th to 17th, respectively), influenced by northerly

425 airflow, regions with high ozone concentrations expanded to the central (Meishan,

426 Ziyang, and Suining) and southwestern (Leshan and Ya'an) parts of the CPUA. In the

427 later stages (August 13th and August 18th), under the influence of northwesterly airflow,

428 regions with high ozone concentrations (Meishan and Leshan) moved southward again,

429 while ozone pollution in other areas of the CPUA gradually weakened. On August 11th

430 to 12th and August 16th to 17th, ozone concentrations in the eight cities of the CPUA

431 reached light pollution levels or higher, with the heaviest pollution recorded on August

432 12th. Specifically, Deyang, Mianyang, Suining, and Meishan reached moderate

433 pollution levels, while Chengdu reached heavy pollution with a concentration of 324

434   μg·m⁻³.
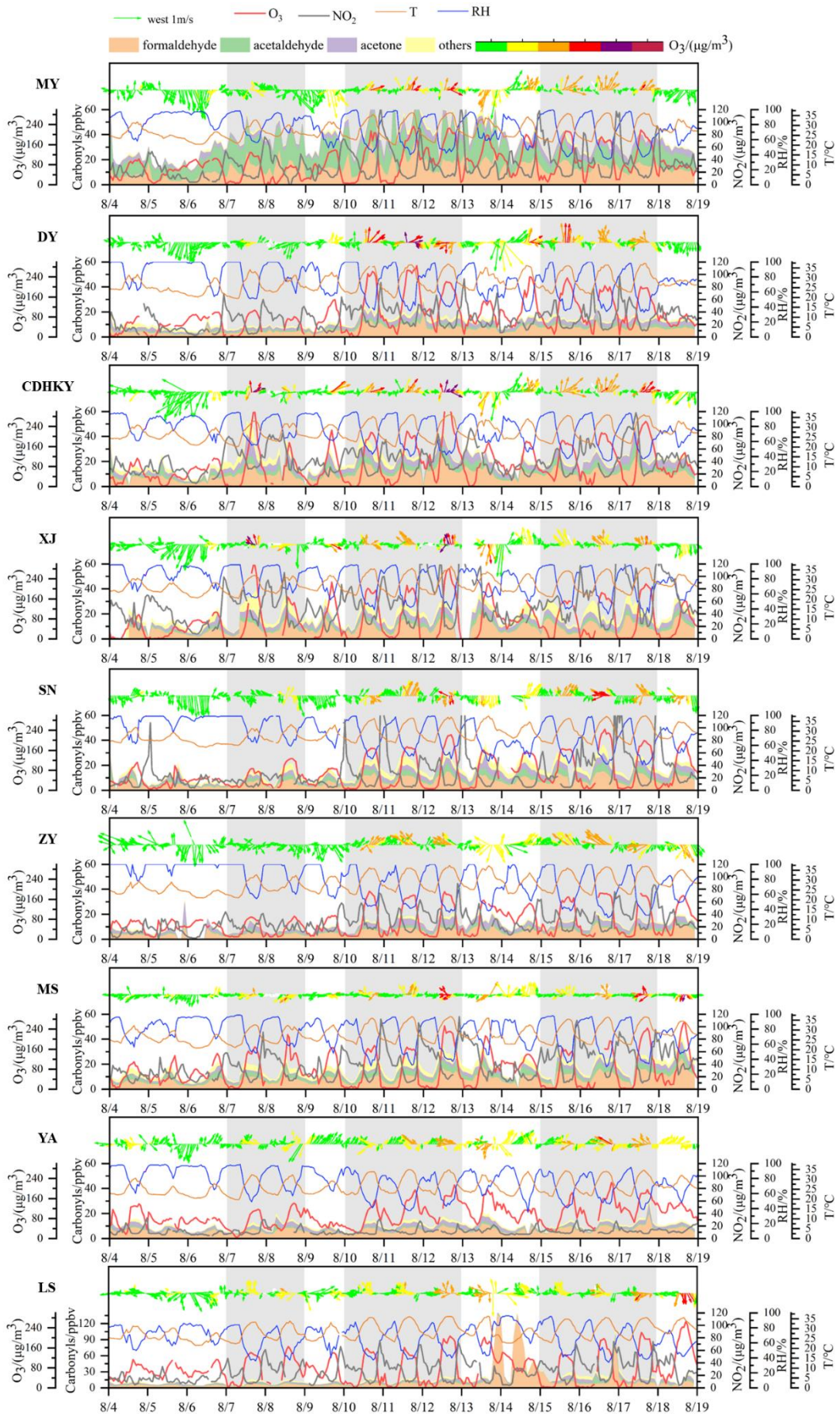
435

436 **Figure 2.** Overview of air quality at each site during the observation period. The gray shaded parts

437 respectively represent the three heavy ozone pollution episodes (EP1, EP2, EP3).
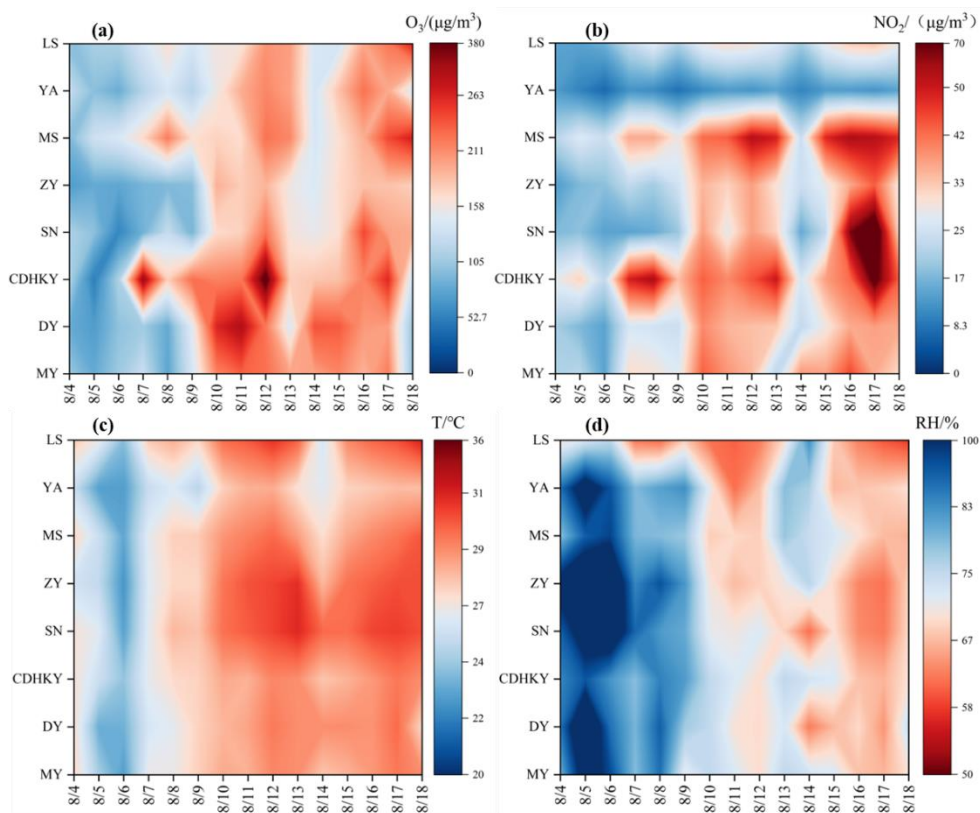
438

439 **Figure 3.** Temporal and spatial variations of (a) ozone concentration, (b) NO_2 concentration, (c)

440 temperature and (d) humidity in the CPUA during the observation period.

441 **3.2 Comparative characterization of carbonyl compounds**

442 **3.2.1 Ambient levels**

443   During the observation period, we utilized 2,4dinitrophenylhydrazine (DNPH)

444 cartridge and high-performance liquid chromatography (HPLC) analysis technique to

445 quantify 15 carbonyl compounds. The concentrations and relative proportions of these

446 compounds are summarized in Table 1. The average total concentration of the 15

447 carbonyls in the CPUA was 17.35 ± 5.31 ppb. Overall, areas with elevated

448 concentrations of carbonyl compounds were primarily concentrated in and around

449 Chengdu in both northern and southern directions. MY site, located to the north of

450 Chengdu, exhibited the highest concentration of carbonyl compounds (35.18 ± 13.37

451   ppb), while YA site, situated southwest of Chengdu, showed the lowest concentration

452   (10.70 ± 4.16 ppb).

453

454   **Table 1.** Daily mean ± standard error of carbonyl compound mixing ratios (ppbv) at each site in

455   the CPUA during the observation period. Sum: the total sum of carbonyl compound mixing ratios

456   across all compounds at each site.

Carbonyls	MY	DY	CDHKY	XJ	SN	ZY	MS	YA	LS
formaldehyde	12.82±6.52	6.06±2.82	10.09±4.21	8.87±4.39	6.98±3.56	5.84±2.69	8.47±4.15	6.36±2.40	6.55±3.35
acetaldehyde	16.65±7.38	1.54±0.77	3.65±2.15	2.33±1.07	2.62±1.74	1.40±0.61	3.24±1.60	0.88±0.68	1.63±1.32
acetone	4.36±1.70	2.80±1.19	4.51±2.25	3.70±1.21	3.14±1.70	3.23±1.73	2.15±1.14	2.18±1.08	2.91±1.63
propionaldehyde	0.41±0.22	0.24±0.14	0.39±0.27	0.39±0.17	0.34±0.22	0.28±0.14	0.41±0.18	0.20±0.15	0.31±0.16
crotoraldehyde	0.20±0.21	0.10±0.11	0.23±0.34	0.05±0.07	0.23±0.08	0.19±0.27	0.15±0.21	0.36±0.24	0.12±0.24
butyaldehyde	0.22±0.48	0.22±0.28	0.40±0.57	0.94±1.67	0.26±0.18	0.06±0.18	0.44±0.46	0.25±0.16	0.02±0.06
benzaldehyde	0.00±0.04	0.02±0.06	0.04±0.11	0.21±0.20	0.08±0.10	0.00±0.01	0.00±0.01	0.00±0.00	0.01±0.04
isovaleraldehyde	0.01±0.14	0.03±0.09	0.08±0.14	0.08±0.13	0.05±0.10	0.01±0.05	0.68±0.42	0.04±0.07	0.06±0.12
valeraldehyde	0.00±0.00	0.25±0.09	0.30±0.59	0.63±0.36	0.85±0.65	0.00±0.00	0.00±0.00	0.00±0.02	0.77±0.47
o-Tolualdehyde	0.46±0.52	0.36±0.29	0.45±0.19	0.00±0.00	0.00±0.00	0.23±0.17	0.43±0.33	0.18±0.22	0.16±0.17
m-Tolualdehyde	0.00±0.02	0.04±0.10	0.04±0.09	0.17±0.17	0.30±0.13	0.00±0.03	0.00±0.02	0.00±0.02	0.01±0.05
p-Tolualdehyde	0.00±0.00	0.01±0.05	0.01±0.04	0.00±0.00	0.00±0.00	0.00±0.00	0.01±0.04	0.00±0.02	0.00±0.02
hexaldehyde	0.00±0.01	0.34±0.25	0.41±0.69	0.57±0.47	0.95±0.65	0.02±0.18	0.78±0.58	0.00±0.01	0.10±0.32
2,5-diemthybenzaldehyde	0.01±0.03	0.00±0.01	0.00±0.01	0.05±0.12	0.00±0.00	0.00±0.01	0.01±0.02	0.00±0.01	0.00±0.01
MACR	0.03±0.20	0.14±0.17	0.26±0.34	1.05±1.10	0.26±0.21	0.19±0.16	0.42±0.36	0.24±0.22	0.81±0.88
Sum	35.18±13.37	12.16±4.84	20.84±8.85	19.04±8.1	16.05±7.73	11.47±4.89	17.19±7.61	10.70±4.16	13.46±6.12

457

458

459

460   Fig.S1 illustrates the relationship between ozone concentration and carbonyl

461 compounds concentration at each site during the observation period. It is evident that

462 the spatial distribution of carbonyl compound concentrations is similar to that of ozone

463 concentration. Regions with severe ozone pollution tend to exhibit higher

464 concentrations of carbonyl compounds. The variation in carbonyl compound

465 concentrations is primarily attributed to anthropogenic emissions and prevailing

466 summer wind directions in the CPUA. Chengdu is the most economically developed

467 city in the CPUA, with notably higher GDP and industrial production values than other

468 regions. Chengdu's major industries include coal-fired power plants, chemical plants,

469 metallurgy and building materials plants, and high concentrations of carbonyls were

470 observed in here. The unique basin climate of the CPUA, characterized by intense

471 sunlight and stable atmospheric conditions, facilitates the accumulation of pollutants.

472 Large amount of industrial emissions and strong photochemical reaction contributes to

473 ozone pollution. Additionally, during the summer, prevailing northerly winds in the

474 CPUA facilitate the downwind transport of pollutants from upwind sources, leading to

475 regional pollution. It is noteworthy that the concentration of carbonyl compounds at the

476 MY site significantly exceeds that at the CDHKY site. Mianyang, with its industrial

477 roots, consistently maintains its position as the second-highest GDP contributor in

478 Sichuan Province. The electronics information industry stands as Mianyang's primary

479 economic driver, constituting approximately half of the city's total output value. Studies

480 investigating the volatile organic compound (VOC) source profile in Chengdu(Zhou et

481 al., 2021) reveal that ethanol and carbonyls predominantly characterize electronics

482 manufacturing emissions.

483 **3.2.2 Compositional characteristics**

484   According to the composition characteristics of 15 carbonyl compounds in the

485 ambient air of each city during the observation period(Table S4). Formaldehyde was

486   the most abundant carbonyl found in these sites followed by acetone and acetaldehyde,

487   which is widely observed in previous studies. The measured ratios of formaldehyde,

488   acetone, and acetaldehyde across different sites ranged from 36.4% to 59.4% (average

489   48.1%), 12.4% to 28.1% (average 19.9%), and 8.2% to 47.3% (average 17.5%),

490   respectively. In this study, the total measured of formaldehyde, acetaldehyde, and

491   acetone(FAT)account for over 78% of the total carbonyls concentrations. At the MY

492   and ZY sites, this proportion even exceeded 90%. It is noteworthy that isobutyraldehyde

493   (MACR) ranks fourth in the volume concentration of 15 carbonyls measured in the

494   ambient air surrounding XJ, accounting for 5.3%. MACR, a characteristic product of

495   isoprene photooxidation from biogenic sources, possibly originates from the abundant

496   vegetation surrounding XJ. It reflects the period's relatively active photochemical

497   reactions, with substantial contributions from secondary formation to the measured

498   carbonyls composition.

499   The observed levels of FAT in different areas were influenced by various factors

500   including sampling period, geographic location, meteorological conditions, chemical

501   removal, and source emissions(Z. Zhang et al., 2016). Despite these influences,

502   comparisons remain valuable in providing an overview of ambient carbonyl levels in

503   the CPUA. During the summer of 2010, a national wide survey of ambient

504   monocarbonyl compounds were conducted simultaneously in nine sites (Ho et al.,

505   2015)found that the total FAT concentration was highest in Chengdu (14.96 ppb),

506   followed by Beijing (11.83 ppb), and Wuhan (11.70 ppb). Beijing, as the capital of

507   China, and Wuhan, being one of the top ten most populous cities in China, played

508   significant roles in this comparison. In our study, the CDHKY site within CPUA

509   exhibited the highest FAT concentration, with values of 18.25 ppb, surpassing those

510   recorded in 2010. Furthermore, the total FAT concentrations observed at the CPUA and

511   XJ sites, with values of 14.99 ppb and 14.90 ppb respectively in our study, closely

512   resemble those reported in August 2010 in Chengdu. The consistently high levels of

513   carbonyl compounds observed in Chengdu, both in 2010 and our current study, indicate

514   that the city likely experiences higher concentrations of these pollutants compared to

515   other regions across the country. However, more extensive temporal data would be

516   beneficial to fully validate this pattern at a national scale. Comparing our findings to

517   international studies, the FAT concentrations at the CDHKY site were lower than those

518   reported in Rio De Janeiro, Brazil(da Silva et al., 2016), during July to October 2013

519   (35.43 ppb), but higher than those in Bangkok, Thailand(Kanjanasiranont et al., 2016b),

520   Orleans, France(Jiang et al., 2016), and the United States(Murillo et al., 2012), with

521   values of 9.05 ppb, 6.12 ppb, and 5.76 ppb, respectively.

522   **3.3 Temporal variations of carbonyl compounds**

523   The diurnal variation of the total mixing ratio of ambient carbonyl compounds and

524   ozone concentration around each site in the CPUA during the observation period is

525   shown in Fig. 4. According to the observation results, the diurnal trend of ozone

526   concentration at each site showed a "unimodal" variation characteristic, that was, it

527   gradually increased from the morning to the peak of one day at noon, and then decreased.

528   The diurnal variation of the total mixing ratio of carbonyl compounds at each site

529   generally showed a characteristic of high during the daytime and low at night. The

530   concentration of carbonyl compounds during the day (6:00-16:00) was 48.8% higher

531   than that at night (18:00-4:00) at the XJ site. This indicated that the concentration of

532   carbonyl compounds increased by photochemical production during the daytime.

533   Additionally, deposition processes, particularly dry deposition at night, likely

534   contribute to the observed diurnal variation in carbonyl levels. The diurnal variation

535   characteristics of each site were different. For example, the diurnal variation

536   characteristics of carbonyl compounds concentration at CDHKY, XJ and SN sites were

537   consistent with those of ozone. The diurnal variation of carbonyl compounds

538   concentrations at other sites showed "double peaks", peaking at 10:00-12:00 and 18:00-

539   20:00, respectively. The concentrations of carbonyl compounds at night were also

540   higher at MY, DY and LS sites. The diurnal minimum values of the total concentration

541   of carbonyl compounds and ozone concentration appeared at similar time, usually at

542   4:00 a.m. or 6:00 a.m. The first peak of the total mixing ratio of carbonyl compounds

543   occurred earlier than the maximum ozone concentration of the day. The first peak of

544   the total mixing ratio of carbonyl compounds mostly occurred between 10:00 and 12:00.

545   And the maximum ozone concentration mostly occurs between 14:00 and 16:00. This

546   was related to the fact that carbonyl compounds were important precursors of ozone.

547   In general, the diurnal variation of the total concentration of carbonyl

548   compounds on pollution days and clean days was high during the daytime and low at

549   night. The total mixing ratio of carbonyl compounds on pollution days was 22.8%-

550   66.2% higher than that on clean days. At the same time, the increase of concentration

551   of carbonyl compounds during the daytime on pollution days was higher than that on

552   clean days. This suggested that the increase in the concentration of carbonyl

553   compounds during the daytime contributed to ozone pollution.
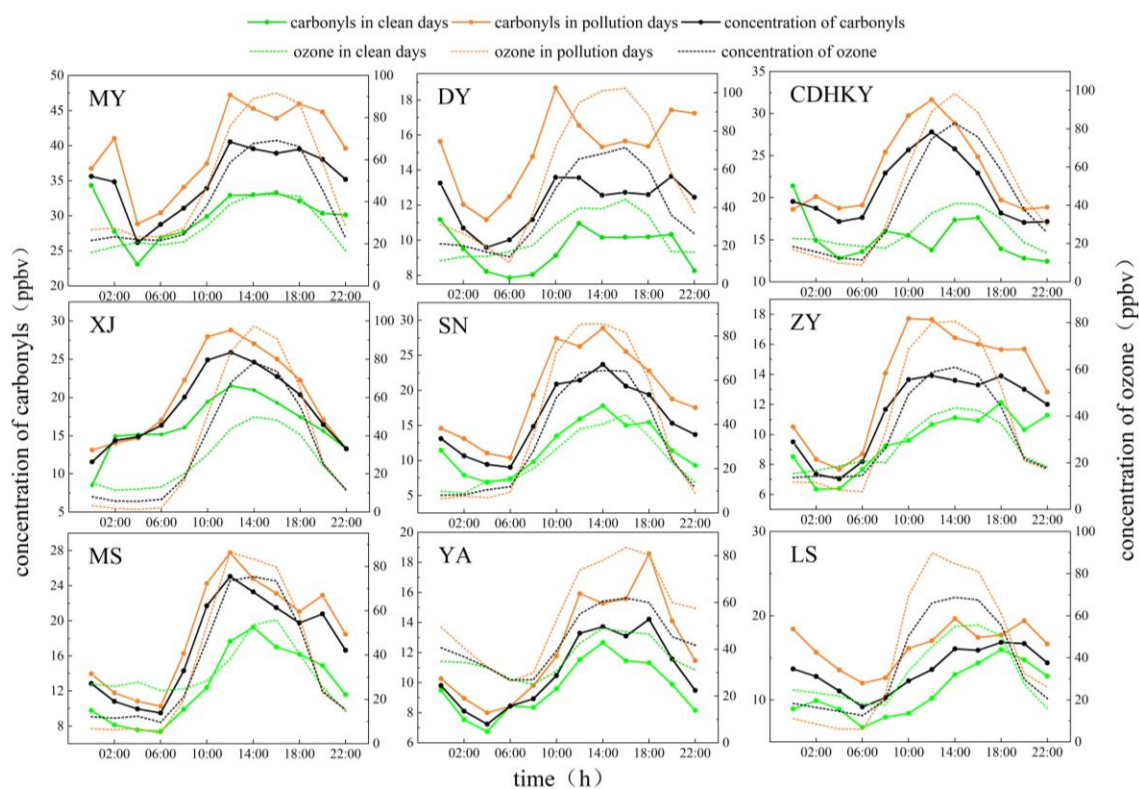
554

555   **Figure 4.** Diurnal variations of carbonyl compounds and ozone concentrations at each site in the

556   CPUA during the observation period

557   **3.4 Atmospheric photochemical reactivity of carbonyl compounds**

558   During the observation period, the total OH radical consumption rate (L_{OH}) and

559   total ozone formation potential (OFP) of the 15 carbonyl compounds at each site are

560   depicted in Fig.5. The ranking of total L_{OH} and total OFP at each site is consistent,

561   except for the YA and ZY sites with lower concentrations of carbonyl compounds,

562   where the atmospheric photochemical reactivity ranking also aligns with the

563   concentration. Among all sites, the MY and CD sites display the highest reactivity,

564   while the YA and ZY sites exhibit the lowest reactivity. During the observation period,

565   carbonyl compounds significantly contributed to ozone formation. The contributions to

566   total VOCs (alkanes, alkenes, alkynes, aromatics, and carbonyl compounds) OFP at the

567   MY, SN, ZY, YA, and LS sites ranged from 19.5% to 48.6%. Formaldehyde and

568   acetaldehyde were identified as the most reactive species in the atmosphere, surpassing

569   other carbonyl compounds in reactivity due to their higher concentrations and inherent

570   reactivity, especially formaldehyde. However, acetone exhibited high inertness and a

571   prolonged atmospheric lifetime, leading to its accumulation in ambient air with

572   concentrations higher than other carbonyl compounds except for formaldehyde and

573   acetaldehyde. Thus, despite its elevated concentration, acetone's reactivity remained

574   relatively low.
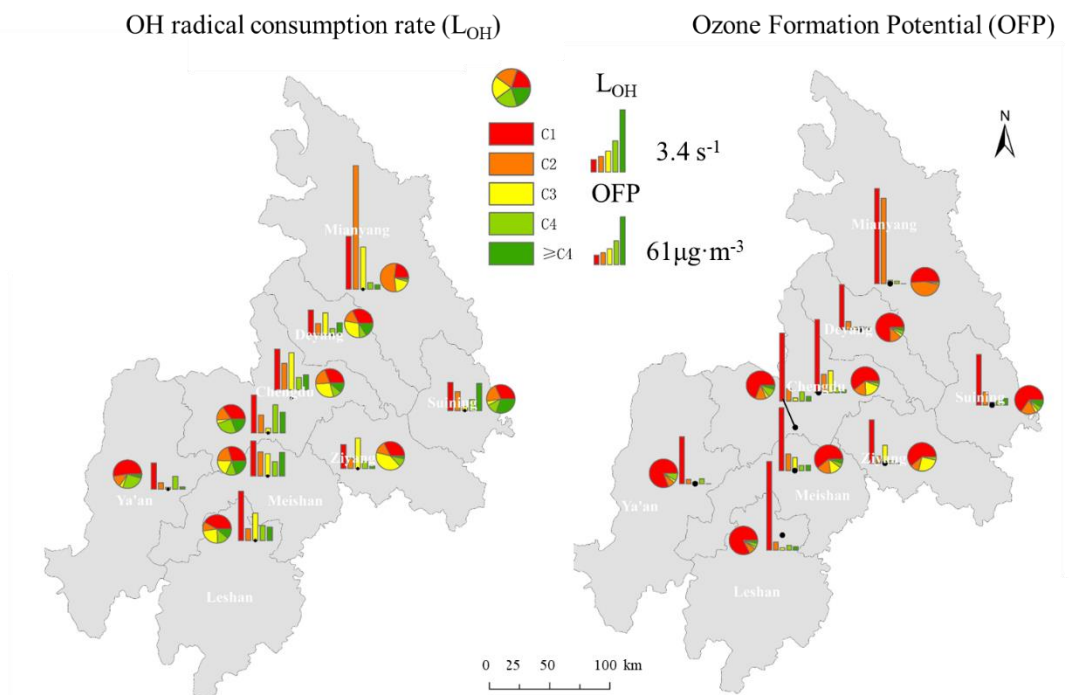
575

576   **Figure 5.** L_{OH} and OFP of carbonyl compounds at each site in the CPUA during the observation

577   period

578   **3.5 Sensitivity analysis of ozone formation based on formaldehyde to NO₂ ratio (FNR)**

579   The change of O_3 formation sensitivity of each site in the CPUA during the

580   observation period is shown in Fig.6. As can be seen from the Fig. 6, most sites remain

581   in the VOCs-limited regime during the cleaning period and EP1 to EP3. Economically

582   developed city such as Chengdu, Meishan, with high levels of formaldehyde and NO_2,

583   remain in the VOCs-limited regime. Ya'an as a city with the lowest GDP ranking in the

584   CPUA, with low levels of formaldehyde and NO_2, remain in the transitional regime.
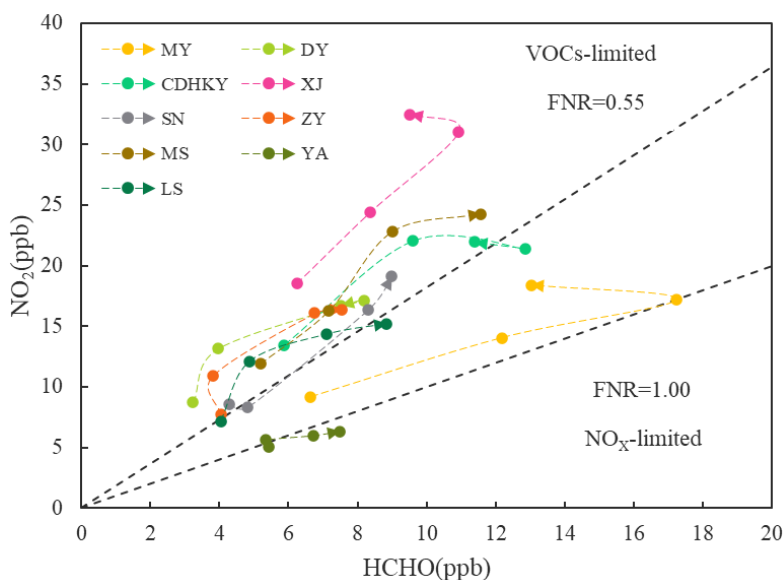
585

586   **Figure 6.** The change of O_3 formation sensitivity of each site in the CPUA during the observation

587   period. The arrows represent time step from clean period to EP1 to EP2 to EP3.

588   The daily variation of O_3 formation sensitivity and ozone concentration at each

589   site in the CPUA during the observation period is shown in Fig. S4. The mean FNR of

590   each site ranged from 0.48 to 1.29 during the observation period. The FNRs were lower

591   than 0.55±0.16 at XJ, DY, ZY, CDHKY, and MS, and higher than 1.0 at LS, SN, YA

592   and MY. At the same time, the mean ozone concentration at each site was between 138

593   and 192 $\mu g \cdot m^{-3}$. The mean ozone concentration in XJ, DY, CDHKY and MS was 166-

594   192 $\mu g \cdot m^{-3}$, it was 150-164 $\mu g \cdot m^{-3}$ in LS, SN, YA and MY. Therefore, it could be seen

595   that most of the sites with high mean ozone concentrations during the observation

596   period, like CDHKY, XJ, MS and Deyan sites, were in the VOCs-limited regime, and

597   most of the stations with low mean ozone concentrations during the observation period

598   such as YA, SN, MY and LS were in the transitional regime. It was worth noting that

599   the mean ozone concentration at ZY site (only 138 $\mu g \cdot m^{-3}$) during the observation

600   period was much lower than that of other sites, but most of the ZY site was in VOCs-

601   limited regime, which was mainly related to the low concentration of formaldehyde. In

602   addition, the FNR value of the MY site was also relatively high, which was mainly

603   caused by the high concentration of formaldehyde.

604   Based on the ratio of formaldehyde to NO_2 mixing ratio, most sites remain in the

605   VOCs-limited regime during the observation period. And the sites with heavy ozone

606   pollution were in the VOCs-limited regime, and the sites with light ozone pollution

607   were in the transitional regime. Photochemical reactivity (L_{OH} and OFP) analysis

608   showed that formaldehyde and acetaldehyde contributed significantly to the

609   enhancement of atmospheric oxidation and ozone formation potential. Therefore, when

610   heavy ozone pollution occurs in the CPUA, special attention should be paid to the

611   control of VOCs, especially formaldehyde and acetaldehyde in carbonyl compounds,

612   under the coordinated control of NOx and VOCs. Overall, this study reveals the

613   important contribution of carbonyl compounds to ozone pollution in the CPUA, and

614   provides scientific support for the establishment of ozone pollution prevention and

615   control measures.

616   **3.6 Source Analysis of carbonyl compounds**

617   **3.6.1 Quantitative source analysis of key carbonyl compounds**

618   The table S7 provides a summary of the background and primary emissions

619   concentrations of formaldehyde, acetaldehyde, and acetone at nine sites across the eight

620   cities of the CPUA, along with the proportion of secondary formation contributing to

621   their concentrations. Background concentrations and primary emissions of

622   formaldehyde, acetaldehyde, and acetone ranged from 50% to 80%, 46% to 83%, and

45% to 78%, respectively. Secondary formation accounted for 20% to 50%, 17% to 54%, and 22% to 55% of their concentrations, respectively. Notably, in SN and YA, the secondary formation of formaldehyde contributed half of the observed concentration, indicating it as the predominant source, while acetaldehyde's secondary formation also prevailed in these sites. Conversely, acetone, with lower reactivity, primarily originated from background concentrations and primary emissions at other sites except YA. Moreover, background concentrations and primary emissions were identified as the main contributors to carbonyl compounds in XJ and LS.

Fig.7 illustrates the secondary formation concentrations of formaldehyde, acetaldehyde, and acetone at each site in the CPUA under both clean and polluted conditions. Under polluted conditions, the secondary concentrations of formaldehyde, acetaldehyde, and acetone exceeded those in clean conditions by 52.4%, 80.3%, and 58.5%, respectively. The most significant increases in secondary concentrations were observed at the SN site, while relatively smaller increases were observed at LS and XJ.
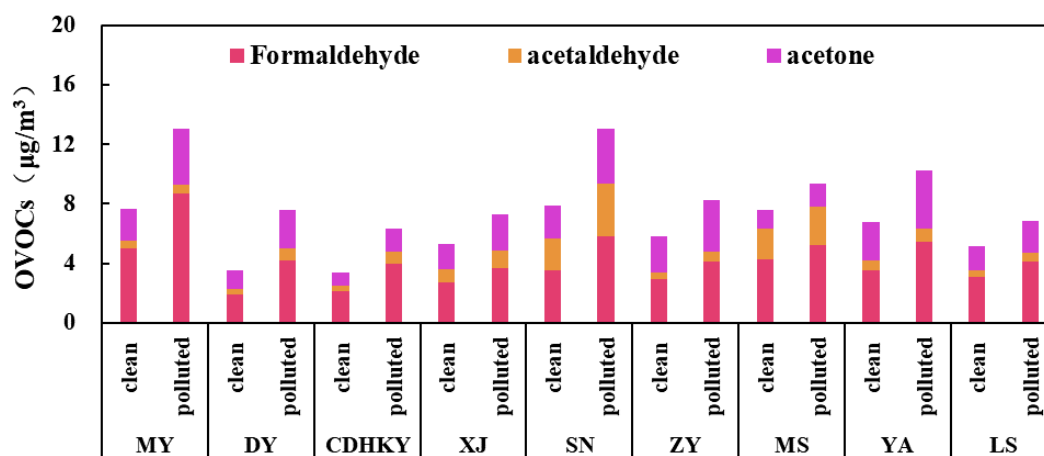
Figure 7. Concentrations of formaldehyde, acetaldehyde and acetone in secondary formation under different pollution conditions at each site in the CPUA during the observation period

3.6.2 Exploration of secondary formation mechanism of key carbonyl compounds

In this study, we utilized VOC data collected on August 11, 12, and 16, when all eight cities in the CPUA were experiencing mild to severe ozone pollution. We calculated the Relative Incremental Reactivity (RIR) of formaldehyde, acetaldehyde,

644 and acetone at the MY, SN, ZY, YA, and LS sites on these days. The OBM analysis

645 allowed us to assess the impact of anthropogenic VOCs (alkanes, alkenes, alkynes,

646 aromatics) and biogenic VOCs (e.g., isoprene) on carbonyl compound formation in the

647 context of regional ozone pollution events (Fig.8). Overall, the sensitivities of different

648 anthropogenic source and plant source VOCs to formaldehyde, acetaldehyde and

649 acetone was consistent among sites. For formaldehyde, reducing alkenes in

650 anthropogenic source VOCs and plant VOCs was the most effective way to control

651 formaldehyde concentration, while reducing alkenes in anthropogenic source VOCs

652 was also beneficial to reduce the formation of acetaldehyde. For acetone with low

653 reactivity, the alkanes in anthropogenic source VOCs were the most sensitive to the

654 formation of acetone, followed by alkenes and BVOCs. Only the RIR value of alkanes

655 were greater than zero, and the RIR values of both alkenes and BVOCs were less than

656 zero, indicating that reducing alkanes could reduce the formation of acetone, while

657 reducing alkenes and BVOCs was not conducive to acetone concentration control.
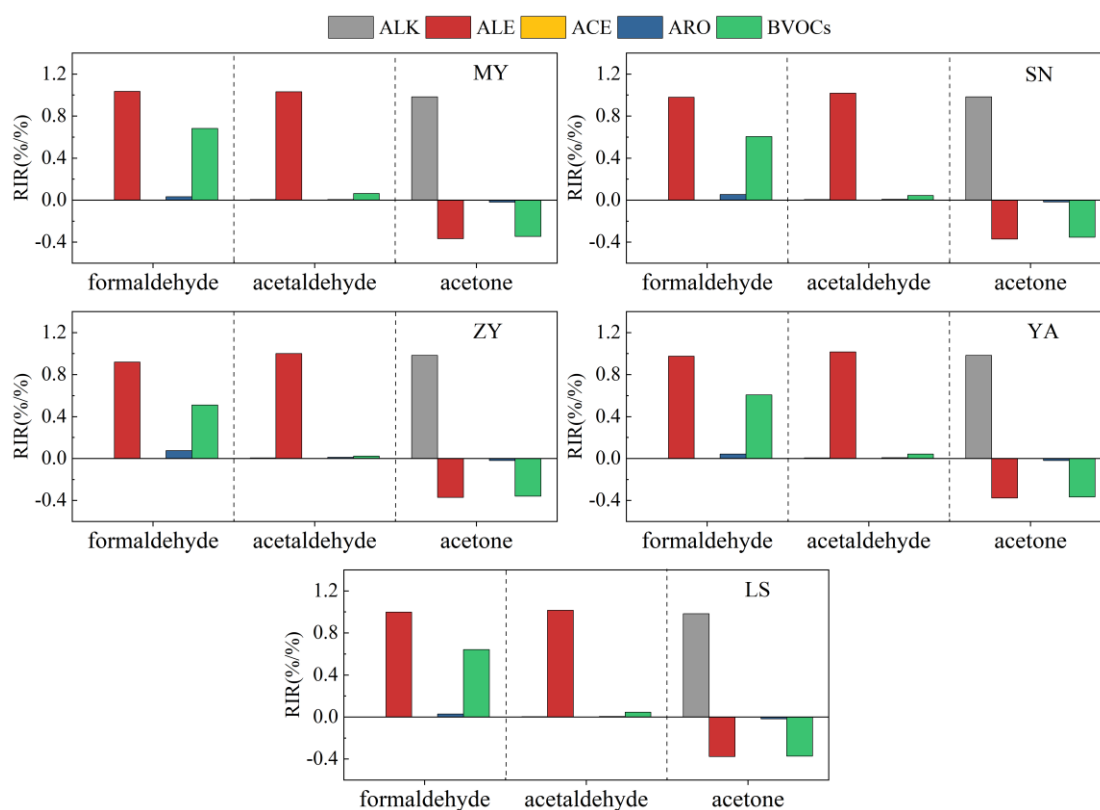
658

659 **Figure 8.** Mean RIRs of formaldehyde, acetaldehyde and acetone to different anthropogenic

660 source VOCs and biogenic source VOCs at MY, SN, ZY, YA and LS sites on August 11th, 12th and

662 **3.6.3 Influence of regional transportation contribution**

663   The TrajStat trajectory model was used to calculate and cluster the 24-hour

664 backward trajectories of air quality at the sampling sites. The backward trajectory

665 during sampling is shown in Fig.S5. During the observation period, the pollution of

666 carbonyl compounds in the cities of the CPUA was affected by the mutual transport

667 among cities in Sichuan Province, especially along the MY-DY-CDHKY route. In

668 addition, the surrounding provinces and cities of Sichuan Province (Gansu and

669 Chongqing) also contributed to the carbonyl compounds of the CPUA.

670   The potential sources of carbonyl compounds at different pollution stages at the

671 CDHKY during the observation period are shown in Fig. 9. It can be seen from the

672 figure that there are differences in the potential sources of carbonyl compounds among

673 different pollution stages at the CDHKY site. The concentration of local carbonyl

674 compounds in CDHKY was high during the early observation period and EP1, which

675 existed local sources, and was also affected by the northern airflow, and carbonyl

676 compounds was also affected by the transport from MY, DY and other northern regions.

677 Under the effect of the continuous northern airflow, the local source emissions

678 decreased during EP1, and the potential source of carbonyl compounds changed to from

679 the junction between CDHKY and ZY. During EP3, under the combined influence of

680 the western airflow, the contribution of transport from SN and ZY to carbonyl

681 compounds increased, while emissions from local sources also increased.
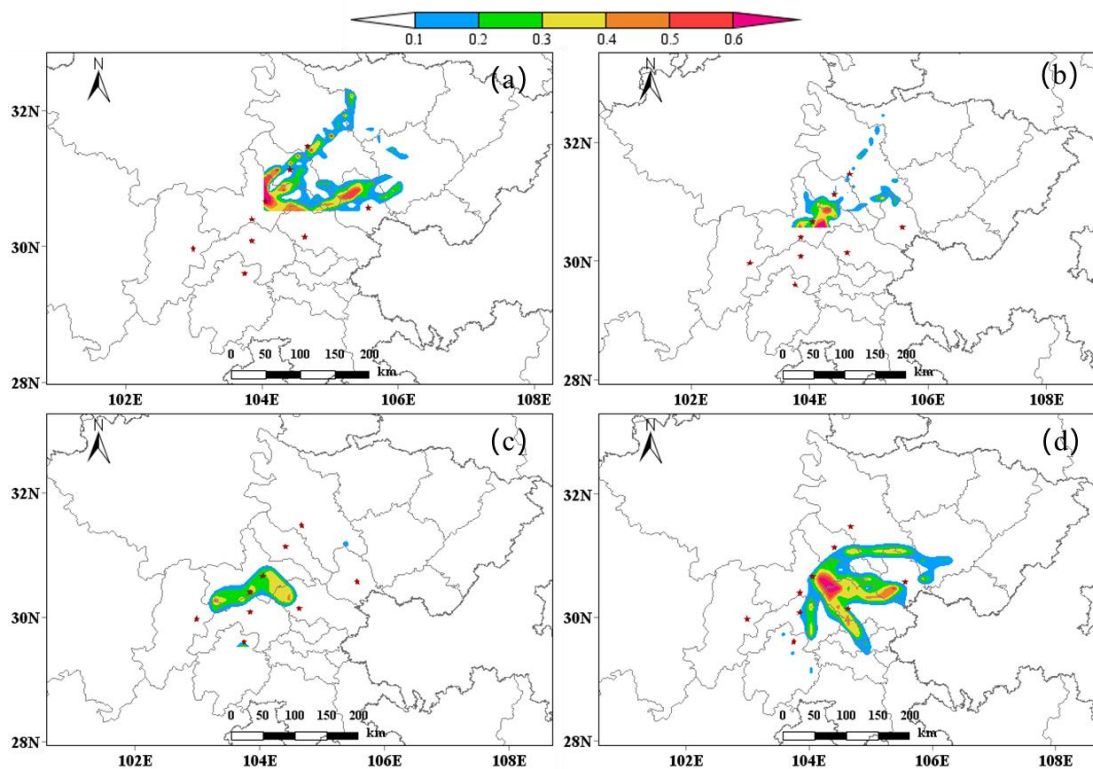
682

683 **Figure 9.** Analysis of potential sources of carbonyl compounds at different periods at the CDHKY

684   site during the observation period (a) August 4th-6th (b) August 7th-9th (c) August 10th-13th (d)

685   August 15th-18th

686 **4. Conclusions**

687   During a concurrent atmospheric observation campaign conducted at nine sites in

688 the CPUA from August 4th to 18th, 2019, three regional heavy ozone pollution episodes,

689 labeled EP1 to EP3, were observed. This study extensively examines the concentration

690 variations, atmospheric chemical reactivity, and sources of carbonyls during this period.

691 The average total concentrations of 15 carbonyl compounds across the nine sites within

692 eight cities of the CPUA were measured at 17.35 ± 5.31 ppb. Spatial analysis revealed

693 a positive correlation between carbonyl levels and ozone concentrations, particularly

694 concentrated around Chengdu in both northern and southern directions. Formaldehyde

695 (36.4%-64.3%), acetone (12.4%-28.1%), and acetaldehyde (8.2%-47.3%) constituted

696 the predominant species by volume concentration. Intriguingly, Chengdu exhibited FAT

697 concentrations surpassing national and international levels, indicating heightened levels

698 compared to other regions. Diurnal variations showed peaks during the day and lows at

699 night, with notable spikes on ozone pollution days. A distinctive "weekend effect" was

700 observed, particularly evident in carbonyl compounds associated with motor vehicle

701 emissions, such as acetaldehyde and acetone, peaking during morning rush hours and

702 nighttime on weekends. This suggests significant contributions from both daytime

703 photochemical processes and nighttime vehicular emissions to carbonyl compounds. At

704 the MY site, 48.6% of the total volatile organic compounds (VOCs) ozone formation

705 potential (OFP) was attributed to the 15 carbonyl compounds, emphasizing their

706 substantial impact on ozone formation, especially formaldehyde and acetaldehyde.

707   Ground-level observations of FNR were utilized to assess the sensitivity of

708 ground-level ozone formation. FNR from ground-level observations were used to

709 determine the sensitivity of ground-level ozone formation. Analysis of FNR revealed

710 that sites experiencing heavy ozone pollution exhibited lower FNRs, indicating a

711 VOCs-limited regime, while sites with lighter ozone pollution were categorized into a

712 transitional regime. Carbonyl compound sources include primary emissions and

713 secondary formation processes. Multivariate linear regression quantitatively analyzed

714 formaldehyde, acetaldehyde, and acetone sources. Secondary formation contributed

715 over 30% on average to formaldehyde, acetaldehyde, and acetone, despite primary

716 emissions being primary sources. OBM modeling revealed that formaldehyde and

717 acetaldehyde primarily originated from the secondary formation of alkenes and BVOCs,

718 while acetone mainly stemmed from the secondary formation of alkanes. Furthermore,

719 it is recommended to establish a scientific control mechanism for both NOx and VOCs,

720 with special attention to formaldehyde, acetaldehyde, and acetone, and their alkenes

721 precursors. Additionally, considering the regional nature of pollution, this study

722 suggests that carbonyl compound pollution is influenced by mutual transport among

723 cities within the CPUA, notably along the MY-DY-CDHKY route. Establishing a

724 collaborative prevention and control mechanism among cities within the CPUA and

725 neighboring provinces and cities is crucial to effectively address carbonyl compounds

726 and ozone pollution in the region in the future.

727

728 **Data availability.** Observational data including meteorological parameters and air

729 pollutants used in this study are available from the corresponding authors upon request

730 (lihong@craes.org.cn).

731

732 **Author contributions.** Hong Li and Jiemeng Bao designed this study. Xin Zhang,

733 Zhenhai Wu, Jiemeng Bao, Li Zhou, Qinwen Tan, and Fumo Yang coordinated the

734 selection of field observation sites, including locations for both VOCs and carbonyls

735 grid sampling. Qinwen Tan and Hefan Liu supported the collection of carbonyls at one

736 site. Zhenhai Wu and Xin Zhang assisted in carbonyls sampling; Xin Zhang and

737 Yunfeng Li assisted in carbonyls sample analysis and data collection. Li Zhou and

738 Hefan Liu organized the analysis of VOCs measurements. Jun Qian, Junhui Chen, and

739 Liqun Deng provided support in project funding application. Jiemeng Bao performed

740 the data analysis and wrote the paper with contributions from all co-authors; Hong Li

741 reviewed the paper, provided comments and finalized it.

742

743 **Competing interests.** The contact author has declared that none of the authors has any

744 competing interests.

745

746 **Acknowledgments.** The authors would like to express their sincere appreciation to

747 Keding Lu and Xin Li of Peking University for their organization of the intensive field

748 observation experiment on the formation mechanisms of photochemical pollution in

749 summer in the CPUA of China. They also want to show their deep gratitude to Yulei

750 Ma, Tianli Song, Xiaodong Wu, Ning Wang, and He Zijun Liu of Sichuan University,

751 as well as Xin Zhang (female) and Hefan Liu of Chengdu Academy of Environmental

752 Protection Sciences for their help in sampling. They are also grateful to Liping Liu of

753 Sichuan Agricultural University in Ya'an City, Kaiyao Lv of Mianyang High-tech Zone

754 Management Committee, Yong Xiao of Deyang Municipal Education Bureau, Ying Ni

755 of Meishan Ecological Environment Bureau, Aihua Zou of Leshan Ecological

756 Environment Bureau, and Chuhan Wang of the Chinese Academy of Environmental

757 Sciences for their substantial support during field observations. Special thanks to Zhen

758 He and Manfei Yin of the Chinese Academy of Environmental Sciences for their

759 assistance in analyzing samples from the XJ site.

760

761 **Financial support.** This research has been supported by the Research Project on

762 Analysis of Multiple Causes of Atmospheric Ozone Pollution in Urban Agglomerations

763 of Chengdu Plain and Development of Management, Prevention, and Control System

764 of Sichuan Academy of Environmental Sciences (No. 510201201905430).

765

766 **References**

767 Altshuller, A. P. (1993). Atmospheric chemistry of VOCs and NOx: Implications for
768   ozone formation. *Environmental Science & Technology*, 27(6), 1104–1117.
769   doi:10.1021/es00043a001

770 Atkinson, R., Arey, J., 2003. Atmospheric Degradation of Volatile Organic Compounds.
771   Chem. Rev. 103, 4605–4638. https://doi.org/10.1021/cr0206420

772 Bao, J., Li, H., Wu, Z., Zhang, X., Zhang, H., Li, Y., Qian, J., Chen, J., Deng, L., 2022.
773   Atmospheric carbonyls in a heavy ozone pollution episode at a metropolis in
774   Southwest China: Characteristics, health risk assessment, sources analysis.
775   Journal of Environmental Sciences 113, 40–54.
776   https://doi.org/10.1016/j.jes.2021.05.029

777 Cardelino, C., Chameides, W., 1995. An observation-based model for analyzing ozone
778   precursor relationships in the urban atmosphere. J. Air Waste Manage. Assoc.
779   45, 161–180.

780 Coggon, M. M., Veres, P. R., Yuan, B., et al. (2019). Emissions of organic carbonyl
781   compounds from biomass burning: A global source of reactive carbon to the
782   atmosphere. *Environmental Science & Technology*, 53(20), 11401–11412.

783 da Silva, D.B.N., Martins, E.M., Corrêa, S.M., 2016. Role of carbonyls and aromatics
784   in the formation of tropospheric ozone in Rio de Janeiro, Brazil. Environ Monit
785   Assess 188, 289. https://doi.org/10.1007/s10661-016-5278-3

786 Duan, J., Guo, S., Tan, J., Wang, S., Chai, F., 2012. Characteristics of atmospheric
787   carbonyls during haze days in Beijing, China. Atmospheric Research 114–115,
788   17–27. https://doi.org/10.1016/j.atmosres.2012.05.010

789   Duan, J., Tan, J., Yang, L., Wu, S., Hao, J., 2008. Concentration, sources and ozone
790   formation potential of volatile organic compounds (VOCs) during ozone
791   episode   in   Beijing.   Atmospheric   Research   88,   25–35.
792   https://doi.org/10.1016/j.atmosres.2007.09.004
793   Fu, T.-M., Jacob, D.J., Wittrock, F., Burrows, J.P., Vrekoussis, M., Henze, D.K., 2008.
794   Global budgets of atmospheric glyoxal and methylglyoxal, and implications for
795   formation of secondary organic aerosols. Journal of Geophysical Research:
796   Atmospheres 113. https://doi.org/10.1029/2007JD009505
797   Fuchs, H., Tan, Z., Lu, K., Bohn, B., Broch, S., Brown, S.S., Dong, H., Gomm, S.,
798   Häseler, R., He, L., Hofzumahaus, A., Holland, F., Li, X., Liu, Y., Lu, S., Min,
799   K.-E., Rohrer, F., Shao, M., Wang, B., Wang, M., Wu, Y., Zeng, L., Zhang,
800   Yinson, Wahner, A., Zhang, Yuanhang, 2017. OH reactivity at a rural site
801   (Wangdu) in the North China Plain: contributions from OH reactants and
802   experimental OH budget. Atmospheric Chemistry and Physics 17, 645–661.
803   https://doi.org/10.5194/acp-17-645-2017
804   Grosjean, D., & Seinfeld, J. H. (1989). Parameterization of the formation potential of
805   secondary organic aerosols. *Atmospheric Environment*, 23(8), 1733–1747.
806   doi:10.1016/0004-6981(89)90058-9
807   Guo, H., Wang, T., Simpson, I.J., Blake, D.R., Yu, X.M., Kwok, Y.H., Li, Y.S., 2004.
808   Source contributions to ambient VOCs and CO at a rural site in eastern China.
809   Atmospheric   Environment   38,   4551–4560.
810   https://doi.org/10.1016/j.atmosenv.2004.05.004
811   Hallquist, M., Wenger, J. C., Baltensperger, U., et al. (2009). The formation, properties,
812   and impact of secondary organic aerosol: Current and emerging issues.
813   *Atmospheric Chemistry and Physics*, 9, 5155–5236. doi:10.5194/acp-9-5155-
814   2009
815   Ho, K.F., Ho, S.S.H., Huang, R.-J., Dai, W.T., Cao, J.J., Tian, L., Deng, W.J., 2015.
816   Spatiotemporal distribution of carbonyl compounds in China. Environmental
817   Pollution 197, 316–324. https://doi.org/10.1016/j.envpol.2014.11.014
818   Hong, Q., Zhu, L., Xing, C., Hu, Q., Lin, H., Zhang, C., Zhao, C., Liu, T., Su, W., Liu,
819   C., 2022. Inferring vertical variability and diurnal evolution of O3 formation
820   sensitivity based on the vertical distribution of summertime HCHO and NO2 in
821   Guangzhou, China. Science of The Total Environment 827, 154045.
822   https://doi.org/10.1016/j.scitotenv.2022.154045
823   Hu, J., Wang, P., Ying, Q., Zhang, H., Chen, J., Ge, X., Li, X., Jiang, J., Wang, S., Zhang,
824   J., Zhao, Y., Zhang, Y., 2017. Modeling biogenic and anthropogenic secondary
825   organic aerosol in China. Atmospheric Chemistry and Physics 17, 77–92.
826   https://doi.org/10.5194/acp-17-77-2017
827   Jiang, Z., Grosselin, B., Daële, V., Mellouki, A., Mu, Y., 2016. Seasonal, diurnal and
828   nocturnal variations of carbonyl compounds in the semi-urban environment of
829   Orléans, France. Journal of Environmental Sciences, Changing Complexity of
830   Air Pollution 40, 84–91. https://doi.org/10.1016/j.jes.2015.11.016

831 Kanjanasiranont, N., Prueksasit, T., Morknoy, D., Tunsaringkarn, T., Sematong, S.,
832   Siriwong, W., Zapaung, K., Rungsiyothin, A., 2016a. Determination of ambient
833   air concentrations and personal exposure risk levels of outdoor workers to
834   carbonyl compounds and BTEX in the inner city of Bangkok, Thailand.
835   Atmospheric   Pollution   Research   7,   268–277.
836   https://doi.org/10.1016/j.apr.2015.10.008
837 Kanjanasiranont, N., Prueksasit, T., Morknoy, D., Tunsaringkarn, T., Sematong, S.,
838   Siriwong, W., Zapaung, K., Rungsiyothin, A., 2016b. Determination of ambient
839   air concentrations and personal exposure risk levels of outdoor workers to
840   carbonyl compounds and BTEX in the inner city of Bangkok, Thailand.
841   Atmospheric   Pollution   Research   7,   268–277.
842   https://doi.org/10.1016/j.apr.2015.10.008
843 Li, N., Fu, T.-M., Cao, J., Lee, S., Huang, X.-F., He, L.-Y., Ho, K.-F., Fu, J.S., Lam, Y.-
844   F., 2013. Sources of secondary organic aerosols in the Pearl River Delta region
845   in fall: Contributions from the aqueous reactive uptake of dicarbonyls.
846   Atmospheric Environment, Improving Regional Air Quality over the Pearl
847   River Delta and Hong Kong: from Science to Policy 76, 200–207.
848   https://doi.org/10.1016/j.atmosenv.2012.12.005
849 Li, Y., Shao, M., Lu, S., Chang, C.-C., Dasgupta, P.K., 2010. Variations and sources of
850   ambient formaldehyde for the 2008 Beijing Olympic games. Atmospheric
851   Environment 44, 2632–2639. https://doi.org/10.1016/j.atmosenv.2010.03.045
852 Ling, Z.H., Zhao, J., Fan, S.J., Wang, X.M., 2017. Sources of formaldehyde and their
853   contributions to photochemical O3 formation at an urban site in the Pearl River
854   Delta,   southern   China.   Chemosphere   168,   1293–1301.
855   https://doi.org/10.1016/j.chemosphere.2016.11.140
856 Liu, J., Li, X., Tan, Z., Wang, W., Yang, Y., Zhu, Y., Yang, S., Song, M., Chen, S., Wang,
857   H., Lu, K., Zeng, L., Zhang, Y., 2021. Assessing the Ratios of Formaldehyde
858   and Glyoxal to NO2 as Indicators of O3–NOx–VOC Sensitivity. Environ. Sci.
859   Technol. 55, 10935–10945. https://doi.org/10.1021/acs.est.0c07506
860 Lou, S., Holland, F., Rohrer, F., Lu, K., Bohn, B., Brauers, T., Chang, C.C., Fuchs, H.,
861   Häseler, R., Kita, K., Kondo, Y., Li, X., Shao, M., Zeng, L., Wahner, A., Zhang,
862   Y., Wang, W., Hofzumahaus, A., 2010. Atmospheric OH reactivities in the Pearl
863   River Delta – China in summer 2006: measurement and model results.
864   Atmospheric   Chemistry   and   Physics   10,   11243–11260.
865   https://doi.org/10.5194/acp-10-11243-2010
866 Luecken, D.J., Hutzell, W.T., Strum, M.L., Pouliot, G.A., 2012. Regional sources of
867   atmospheric formaldehyde and acetaldehyde, and implications for atmospheric
868   modeling.   Atmospheric   Environment   47,   477–490.
869   https://doi.org/10.1016/j.atmosenv.2011.10.005
870 Lui, K.H., Ho, S.S.H., Louie, P.K.K., Chan, C.S., Lee, S.C., Hu, D., Chan, P.W., Lee,
871   J.C.W., Ho, K.F., 2017. Seasonal behavior of carbonyls and source
872   characterization of formaldehyde (HCHO) in ambient air. Atmospheric

873   Environment 152, 51–60. https://doi.org/10.1016/j.atmosenv.2016.12.004

874 Monks, P. S., Archibald, A. T., Colette, A., Cooper, O., Coyle, M., Derwent, R., ... &
875   Williams, M. L. (2015). Tropospheric ozone and its precursors from the urban
876   to the global scale from air quality to short-lived climate forcer. *Atmospheric*
877   *Chemistry and Physics*, 15(15), 8889-8973.

878 Murillo, J.H., Marín, J.F.R., Román, S.R., 2012. Determination of carbonyls and their
879   sources in three sites of the metropolitan area of Costa Rica, Central America.
880   Environ Monit Assess 184, 53–61. https://doi.org/10.1007/s10661-011-1946-5

881 Pang, X., Mu, Y., 2006. Seasonal and diurnal variations of carbonyl compounds in
882   Beijing ambient air. Atmospheric Environment 40, 6313–6320.
883   https://doi.org/10.1016/j.atmosenv.2006.05.044

884 Rao, Z., Chen, Z., Liang, H., Huang, L., Huang, D., 2016. Carbonyl compounds over
885   urban Beijing: Concentrations on haze and non-haze days and effects on radical
886   chemistry. Atmospheric Environment, Air Pollution in the Beijing – Tianjin –
887   Hebei (BTH) region, China 124, 207–216.
888   https://doi.org/10.1016/j.atmosenv.2015.06.050

889 Sahu, L. K., & Saxena, P. (2015). High time-resolved volatile organic compounds
890   measurements at an urban location in India: Sources, variability, and role in
891   ozone formation. *Environmental Science and Pollution Research*, 22(5), 3975-
892   3986.

893 Schroeder, J.R., Crawford, J.H., Fried, A., Walega, J., Weinheimer, A., Wisthaler, A.,
894   Müller, M., Mikoviny, T., Chen, G., Shook, M., Blake, D.R., Tonnesen, G.S.,
895   2017. New insights into the column CH2O/NO2 ratio as an indicator of near-
896   surface ozone sensitivity. Journal of Geophysical Research: Atmospheres 122,
897   8885–8907. https://doi.org/10.1002/2017JD026781

898 Shao, M., Lu, S., Liu, Y., Xie, X., Chang, C., Huang, S., Chen, Z., 2009. Volatile organic
899   compounds measured in summer in Beijing and their role in ground-level ozone
900   formation. Journal of Geophysical Research: Atmospheres 114.
901   https://doi.org/10.1029/2008JD010863

902 Shen, X., Zhao, Y., Chen, Z., Huang, D., 2013. Heterogeneous reactions of volatile
903   organic compounds in the atmosphere. Atmospheric Environment 68, 297–314.
904   https://doi.org/10.1016/j.atmosenv.2012.11.027

905 Tan, Z., Lu, K., Jiang, M., Su, R., Dong, H., Zeng, L., Xie, S., Tan, Q., Zhang, Y., 2018.
906   Exploring ozone pollution in Chengdu, southwestern China: A case study from
907   radical chemistry to O3-VOC-NOx sensitivity. Science of The Total
908   Environment 636, 775–786. https://doi.org/10.1016/j.scitotenv.2018.04.286

909 Tonnesen, G.S., Dennis, R.L., 2000. Analysis of radical propagation efficiency to assess
910   ozone sensitivity to hydrocarbons and NO x : 2. Long-lived species as indicators
911   of ozone concentration sensitivity. Journal of Geophysical Research:
912   Atmospheres 105, 9227–9241. https://doi.org/10.1029/1999JD900372

913 Vermeuel, M.P., Novak, G.A., Alwe, H.D., Hughes, D.D., Kaleel, R., Dickens, A.F.,
914   Kenski, D., Czarnetzki, A.C., Stone, E.A., Stanier, C.O., Pierce, R.B., Millet,

915   D.B., Bertram, T.H., 2019. Sensitivity of Ozone Production to NOx and VOC
916   Along the Lake Michigan Coastline. Journal of Geophysical Research:
917   Atmospheres 124, 10989–11006. https://doi.org/10.1029/2019JD030842

918 Wang, C., Huang, X.-F., Han, Y., Zhu, B., He, L.-Y., 2017. Sources and Potential
919   Photochemical Roles of Formaldehyde in an Urban Atmosphere in South China.
920   Journal of Geophysical Research: Atmospheres 122, 11,934-11,947.
921   https://doi.org/10.1002/2017JD027266

922 Wang, Y., Guo, H., Zou, S., Lyu, X., Ling, Z., Cheng, H., Zeren, Y., 2018. Surface O3
923   photochemistry over the South China Sea: Application of a near-explicit
924   chemical mechanism box model. Environmental Pollution 234, 155–166.
925   https://doi.org/10.1016/j.envpol.2017.11.001

926 Wang, Y., Wang, H., Zhang, X., et al. (2020). Formation of secondary organic aerosols
927   from carbonyl compounds: Insights from field observations and simulations.
928   *Atmospheric Chemistry and Physics*, 20, 6177–6189.

929 Xue, L., Gu, R., Wang, T., Wang, X., Saunders, S., Blake, D., Louie, P.K.K., Luk,
930   C.W.Y., Simpson, I., Xu, Z., Wang, Z., Gao, Y., Lee, S., Mellouki, A., Wang, W.,
931   2016. Oxidative capacity and radical chemistry in the polluted atmosphere of
932   Hong Kong and Pearl River Delta region: analysis of a severe photochemical
933   smog episode. Atmospheric Chemistry and Physics 16, 9891–9903.
934   https://doi.org/10.5194/acp-16-9891-2016

935 Xue, L.K., Wang, T., Gao, J., Ding, A.J., Zhou, X.H., Blake, D.R., Wang, X.F., Saunders,
936   S.M., Fan, S.J., Zuo, H.C., Zhang, Q.Z., Wang, W.X., 2014. Ground-level ozone
937   in four Chinese cities: precursors, regional transport and heterogeneous
938   processes. Atmospheric Chemistry and Physics 14, 13175–13188.
939   https://doi.org/10.5194/acp-14-13175-2014

940 Xue, L.K., Wang, T., Guo, H., Blake, D.R., Tang, J., Zhang, X.C., Saunders, S.M., Wang,
941   W.X., 2013. Sources and photochemistry of volatile organic compounds in the
942   remote atmosphere of western China: results from the Mt. Waliguan
943   Observatory. Atmospheric Chemistry and Physics 13, 8551–8567.
944   https://doi.org/10.5194/acp-13-8551-2013

945 Xue, L., Wang, T., Louie, P. K. K., Luk, C. W. Y., Blake, D. R., Gao, J., & Lee, S. H.
946   (2013). Increasing external effects negate local efforts to control ozone air
947   pollution: A case study of Hong Kong and implications for other Chinese cities.
948   Environmental Science & Technology, 47(17), 10299-10305.

949 Yang, X., Xue, L., Wang, T., Wang, X., Gao, J., Lee, S., Blake, D.R., Chai, F., Wang,
950   W., 2018. Observations and Explicit Modeling of Summertime Carbonyl
951   Formation in Beijing: Identification of Key Precursor Species and Their Impact
952   on Atmospheric Oxidation Chemistry. Journal of Geophysical Research:
953   Atmospheres 123, 1426–1440. https://doi.org/10.1002/2017JD027403

954 Yang, X., Xue, L., Yao, L., Li, Q., Wen, L., Zhu, Y., Chen, T., Wang, X., Yang, L., Wang,
955   T., Lee, S., Chen, J., Wang, W., 2017. Carbonyl compounds at Mount Tai in the
956   North China Plain: Characteristics, sources, and effects on ozone formation.

Atmospheric Research 196, 53–61. https://doi.org/10.1016/j.atmosres.2017.06.005

Ye, Z., Xie, S., Wu, Y., et al. (2021). Characterization of carbonyl compounds and their contributions to ozone and secondary organic aerosol formation in a megacity. *Environmental Science & Technology*, 55(14), 9465–9474.

Yuan, B., Chen, W., Shao, M., Wang, M., Lu, S., Wang, Bin, Liu, Y., Chang, C.-C., Wang, Boguang, 2012. Measurements of ambient hydrocarbons and carbonyls in the Pearl River Delta (PRD), China. Atmospheric Research, Remote Sensing of Clouds and Aerosols: Techniques and Applications - Atmospheric Research 116, 93–104. https://doi.org/10.1016/j.atmosres.2012.03.006

Zhang, X., Chen, Z.M., Zhao, Y., 2010. Laboratory simulation for the aqueous OH-oxidation of methyl vinyl ketone and methacrolein: significance to the in-cloud SOA production. Atmospheric Chemistry and Physics 10, 9551–9561. https://doi.org/10.5194/acp-10-9551-2010

Zhang, X., Wu, Z., He, Z., Zhong, X., Bi, F., Li, Y., Gao, R., Li, H., Wang, W., 2022. Spatiotemporal patterns and ozone sensitivity of gaseous carbonyls at eleven urban sites in southeastern China. Science of The Total Environment 824, 153719. https://doi.org/10.1016/j.scitotenv.2022.153719

Zhang, Y., Wang, X., Wen, S., Herrmann, H., Yang, W., Huang, X., Zhang, Z., Huang, Z., He, Q., George, C., 2016. On-road vehicle emissions of glyoxal and methylglyoxal from tunnel tests in urban Guangzhou, China. Atmospheric Environment 127, 55–60. https://doi.org/10.1016/j.atmosenv.2015.12.017

Zhang, Z., Zhang, Y., Wang, X., Lü, S., Huang, Z., Huang, X., Yang, W., Wang, Y., Zhang, Q., 2016. Spatiotemporal patterns and source implications of aromatic hydrocarbons at six rural sites across China's developed coastal regions. Journal of Geophysical Research: Atmospheres 121, 6669–6687. https://doi.org/10.1002/2016JD025115

Zhou, Z., Tan, Q., Deng, Y., Lu, C., Song, D., Zhou, X., Zhang, X., Jiang, X., 2021. Source profiles and reactivity of volatile organic compounds from anthropogenic sources of a megacity in southwest China. Science of The Total Environment 790, 148149. https://doi.org/10.1016/j.scitotenv.2021.148149